Conversion between CIELAB and Munsell Hue

3 authors:

Forough Mahyar
Institute for Color Science and Technology (I…

Stephen Westland
University of Leeds

Vien Cheung
University of Leeds

doi: 10.1111/j.1478-4408.2010.00224.x

Different transformation methods between CIELAB coordinates and Munsell hue

Coloration Technology

Society of Dyers and Colourists

Forough Mahyar, Vien Cheung and Stephen Westland*

School of Design, University of Leeds, Leeds LS2 9JT, UK
Email: s.westland@leeds.ac.uk

Received: 4 June 2009; Accepted: 4 December 2009

This research aims to convert CIE $L^*C^*_{ab}h_{ab}$ coordinates into corresponding Munsell hues. Different transformation methods for colour mapping from CIELAB colour space to Munsell hues are proposed. Polynomial equations that predict Munsell hue from CIELAB h_{ab} suffer from poor performance as there is no direct one-to-one mapping. Polynomial methods that predict Munsell hue from all three $L^*C^*_{ab}h_{ab}$ values also show limited performance. However, a distance-weighted look-up-table model based upon the CIEDE2000 colour-difference equation is able to predict Munsell hue to an accuracy of 1 unit of root mean square error. All transformation methods in this paper were developed using CIE illuminant C and the 2° standard observer conditions and were based on 2729 Munsell renotation colour samples.

Introduction

Colour-space metrics have been deeply and widely investigated in recent decades and still are being currently researched. Extensive work has been carried out to transform between Munsell space and other spaces [1–16]. The Munsell colour system has three fundamental orthogonal attributes called Munsell hue, Munsell chroma and Munsell value. In terms of CIE spaces (CIE XYZ and CIELAB), there has been focus on the relationship between Munsell value and CIE luminance Y; however, there has been rather less focus on finding the relationship between Munsell colour coordinates and CIE $L^*C^*_{ab}h_{ab}$ colour coordinates. One of the reasons why a transformation for this relationship is desirable is to enable a comparison of visual data between the two colour spaces; for example, the authors' work on the investigation of complementary colour harmony [17]. Some preliminary results from this study have already been published by the authors [18]. This work considers several approaches to convert CIE $L^*C^*_{ab}h_{ab}$ coordinates to Munsell hues.

Newhall [1] originated a psychophysical method in order to obtain Munsell hue and chroma from graphical interpolation of chromaticity coordinates of Munsell data plotted for each value steps. He also focused on the relationship between CIE luminance Y and Munsell value V by drawing different charts and plots. The first conversion method (implemented as a software program for a high-speed digital computer) between CIE Y*xy* data and Munsell HVC was published in 1960 by Rheinboldt and Menard [2]. In this method, search and interpolation procedures were applied in order to find the closest Munsell data to the sample specified in Y*xy*. In the study by Rheinboldt and Menard, the existing Munsell data were extrapolated in order to give more data that are estimates and have never been validated as real surface colours. Fifth-order polynomials to compute V from Y were found by McCamy [3] to be an accurate method resulting in maximum errors of 0.0035 in Munsell values. However, inversion of this polynomial is not trivial. Simon and Frost [4] used interpolation to transform between CIE colorimetric data and Munsell notations, but the interpolation was only shown to be effective on a relatively small limited range around the samples. The transformation between RGB and HVC was investigated by Miahara and Yoshida [5]. However, the method was on the basis of multiple regression analysis of just 250 colour samples. Some research has also been carried out to investigate the relationship between reflectance spectra and Munsell notations [6,7]. A conversion method has been developed through a new colour space, proposed by Nayatani [8]. Further related studies can be found from the references of this publication [9–16].

Experimental

In this study, 2729 Munsell renotation colours were considered in order to evaluate the proposed transformations. The notation was developed in 1905 by Albert H Munsell and the atlas was released in 1915 and commercialised in 1929. Prior to 1943, the Munsell system was defined by the physical samples and thus the basic specification of the Munsell system was the spectral reflectance function of each colour chip. The spacing of the chips was intensively studied by the colorimetry committee of the Optical Society of America and in 1943 the CIE tristimulus values of ideally spaced chips were published as the Munsell Renotation System [19]. Each colour with corresponding Munsell HVC values was specified in terms of 1931 chromaticity coordinates *xy* and luminance factors Y. Note, however, that none of the data should be confused with actual measurements from the Munsell colour book [20]. The data contains the real colours only, 'real' being those lying inside the MacAdam limits. Specifically, these are those colours listed in the original 1943 renotation articles [1].

All transformation methods have been developed for CIE illuminant C and the 2° standard observer conditions. It is worth noting that, as the primary step for the transformations, all numeric alphabetic Munsell hues were converted to numeric values between 0 and 100. For example, in this experiment, the Munsell hue identifier of '10RP' was converted into 100. Evidently, with the multiplications of those values by 3.6, all of the angles will be mapped in the range of 0° and 360° (analogous to

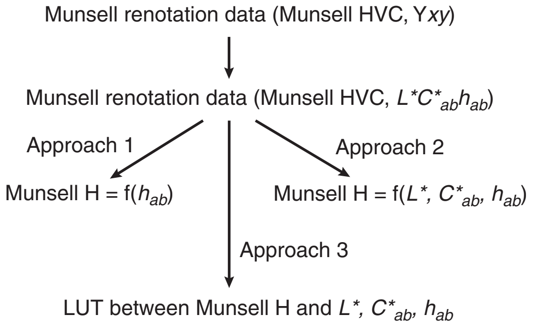

Figure 1 Flow chart of different applied transformation methods between Munsell and CIELAB colour spaces

CIELAB). The Y*xy* values were converted to XYZ which easily allows the subsequent calculation of $L^*a^*b^*$ or $L^*C^*_{ab}h_{ab}$ values. The chart in Figure 1 shows all applied methods in this work.

The research programme involved the investigation and comparative analysis of different transformation methods:

- Approach 1: fitting polynomial transforms to the Munsell renotation data between Munsell hue and CIE h_{ab};
- Approach 2: fitting polynomial transforms to the Munsell renotation data between Munsell hue and CIE $L^*C^*_{ab}h_{ab}$;
- Approach 3: Building up a look-up table (LUT) between $L^*C^*_{ab}h_{ab}$ and Munsell hue.

Approach 1

In this section, various polynomial models are used in an attempt to predict Munsell hue from CIE hue. Eqns 1–4 list the first-, second-, third- and fourth-order polynomial relationships that were used.

$$\mathrm{H} = a_1h_{ab} + b_1 \tag{1}$$

$$\mathrm{H} = a_2h_{ab}^2 + b_2h_{ab} + c_2 \tag{2}$$

$$\mathrm{H} = a_3h_{ab}^3 + b_3h_{ab}^2 + c_3h_{ab} + d_3 \tag{3}$$

$$\mathrm{H} = a_4h_{ab}^4 + b_4h_{ab}^3 + c_4h_{ab}^2 + d_4h_{ab} + e_4 \tag{4}$$

In each case, the coefficients of the equations were optimised to minimise the root square mean (RMS) error between actual and predicted H values.

Approach 2

The relationship between Munsell hue and CIE hue is not a simple one-to-one mapping. The same CIE hue can map to different values of Munsell hue depending upon the CIELAB chroma and lightness values. Therefore, Approach 1 is necessarily of limited value and so, in Approach 2, we consider various polynomial relationships between the three CIELAB values (L^*, C^*_{ab} and h_{ab}) and Munsell hue.

Eqns 5–7 detail the polynomial relationships (first-, second- and third-order) that have been evaluated.

$$\mathrm{H} = a_5L^* + b_5C^*_{ab} + c_5h_{ab} + d_5 \tag{5}$$

$$\begin{aligned}\mathrm{H} = {} & a_6L^* + b_6C^*_{ab} + c_6h_{ab} + d_6L^{*2} + e_6{C^*_{ab}}^2 + f_6h_{ab}^2 \\ & + g_6L^*C^*_{ab} + j_6L^*h_{ab} + k_6C^*_{ab}h_{ab} + m_6\end{aligned} \tag{6}$$

$$\begin{aligned}\mathrm{H} = {} & a_7L^* + b_7C^*_{ab} + c_7h_{ab} + d_7L^{*2} + e_7{C^*_{ab}}^2 + f_7h_{ab}^2 \\ & + g_7L^{*3} + j_7{C^*_{ab}}^3 + k_7h_{ab}^3 + m_7L^{*2}C^*_{ab} + n_7L^{*2}h_{ab} \\ & + p_7{C^*_{ab}}^2h_{ab} + r_7{C^*_{ab}}^2L^* + s_7h_{ab}^2L^* + t_7h_{ab}^2C^*_{ab} \\ & + u_7L^*C^*_{ab}h_{ab} + w_7\end{aligned} \tag{7}$$

Approach 3

A distance-weighted interpolation look-up-table (LUT) model between all CIE coordinates $L^*C^*_{ab}h_{ab}$ and the corresponding Munsell hue has been applied in Approach 3. This technique was selected, rather than tetrahedral interpolation [21], because the latter requires a uniform distribution of samples. To construct the LUT, the selection of eight samples around the target with known CIELAB values was made. The choice of eight samples to use for the interpolation was somewhat arbitrary, but based on some preliminary investigation using 6, 8, 10 and 12 closest neighbours. In order to determine closeness, the distance between the target and each of the 2729 samples was calculated on the basis of three different criteria:

- M-1: the smallest Euclidean distance in CIELAB space (ΔE^*_{ab});
- M-2: the smallest Euclidian distance in XYZ space (ΔE_{xyz});
- M-3: the smallest CIEDE2000 colour difference (ΔE_{00}).

The reason that we consider closeness in different spaces and using different metrics is that it is established that the CIELAB formula is not a very good representation of the Munsell psychological space for colours [22].

For each aforementioned method, the measured distances between the eight selected samples and the target were used to compute weights (ω) on the basis of the following inverse power law weighted function (Eqns 8 and 9). The weights vary inversely with the distance (d) between each of the eight points and the target point, thus:

$$\sigma_i = 1/(d_i^{\mu} + \varepsilon) \tag{8}$$

$$\omega_i = \sigma_i / \sum \sigma_i \tag{9}$$

The parameters μ and ε in Eqn 9 affect the locality of the regression [23,24] and are then used to generate weights that allow the estimation of Munsell hue (10):

$$\text{Predicted Munsell hue} = \sum \omega_i H_i \tag{10}$$

where H_i is the identified Munsell hue of each of the eight selected points. However, it is not obvious what the values of the parameters μ and ε should be. Therefore, different values of the parameters were tested and used to predict Munsell hue for each of the 2729 Munsell

Table 1 Optimised values for parameters μ and ε on the basis of the eight closest samples

	ΔE^*_{ab}	ΔE_{xyz}	ΔE_{00}
μ	1.8550	4.5266	3.7813
ε	0.1369	0.1354	1.6742

samples in turn, and the parameters that resulted in the best predictions were recorded and are noted in Table 1. Note that this optimisation was required using each of the three spaces that were considered separately.

Results and Discussion

The transformation method between CIELAB and Munsell colour spaces was performed in various ways, fitting a polynomial equation to the Munsell renotation data between Munsell hues and CIE hues (Approach 1), fitting a polynomial equation to the Munsell renotation data between Munsell hues and CIE coordinates (Approach 2) and constructing the LUT method between the CIELAB coordinates and Munsell hues (Approach 3). Figures 2–5 illustrate the results obtained from Approach 1. The symbols in the figures show the data points and the fitted polynomial equations are shown as solid lines. It is evident from these figures that there is no simple one-to-one mapping between Munsell hue and CIE h_{ab}. It therefore seems unlikely that Approach 1 could be successful in terms of an effective transformation method. The other colour coordinates (chroma and lightness) must be considered or a more complex LUT approach used. However, another problem with Approach 1 is the lack of continuity that arises from the circular nature of hue. Thus, a hue of 350°, for example, could be considered to be a hue of −10°.

The magnified sections of Figures 2–5 illustrate the degree of continuity by considering the predictions of the models in the vicinity of 0° and for hues that are considered to be slightly smaller than 0° (i.e. negative). It is evident that the first-, second- and fourth-order models display considerable lack of continuity. Only the third-order model demonstrates reasonable continuity (whether we consider a hue to be 359° or −1°, for example, we obtain similar predictions). Table 2 lists the coefficients that were determined for each of the models that were tested.

Although an inspection of Figures 2–5 is interesting, we have used a quantitative method to assess performance of the various approaches. A leave-one-out prediction error method has been used for all 2729 Munsell renotation samples. In the leave-one-out prediction error method, one of the 2729 samples was considered as a test sample

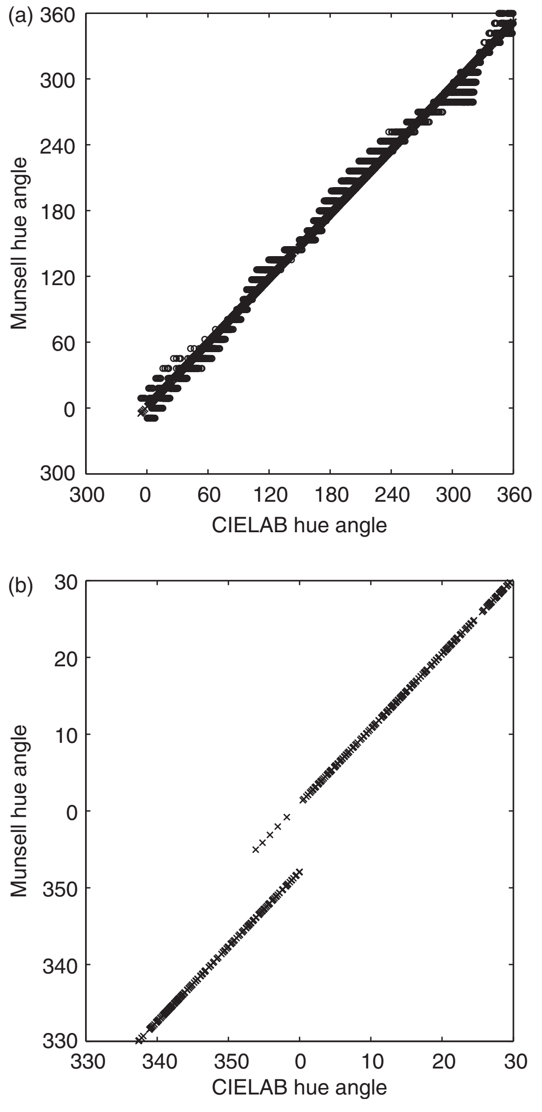

Figure 2 (a) Munsell hue angles against CIELAB hue angles with best-fit linear relationship (Eqn 1) and (b) magnified image

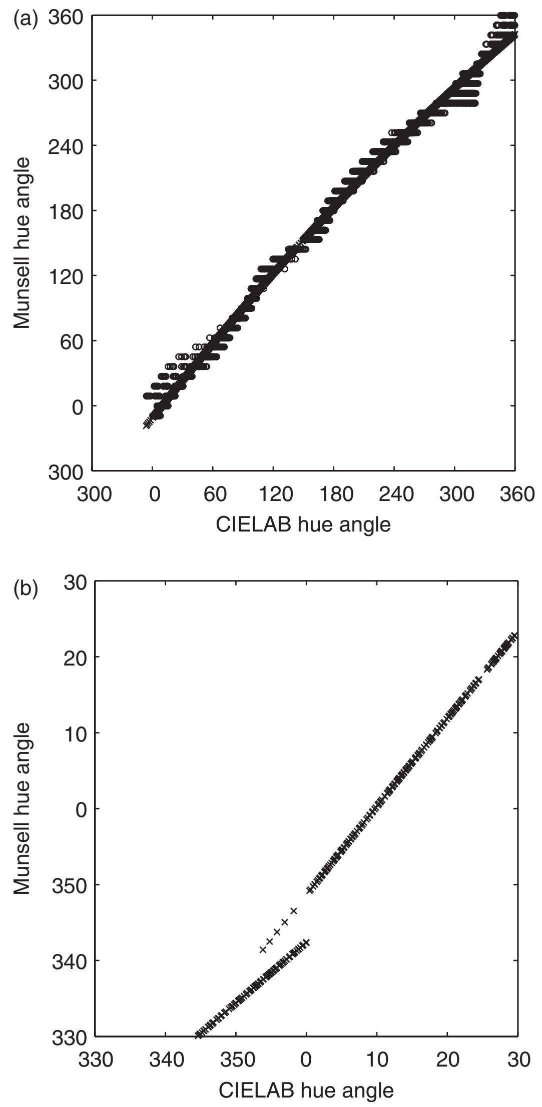

Figure 3 (a) Munsell hue angles against CIELAB hue angles with fitting a second-order polynomial (Eqn 2) and (b) magnified image

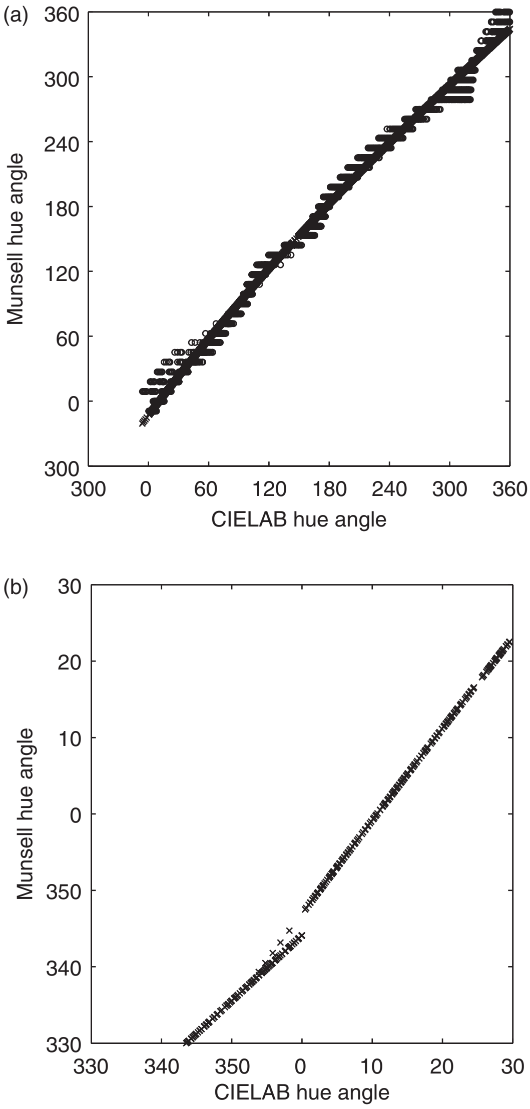

Figure 4 (a) Munsell hue angles against CIELAB hue angles with fitting a third-order polynomial (Eqn 3) and (b) magnified image

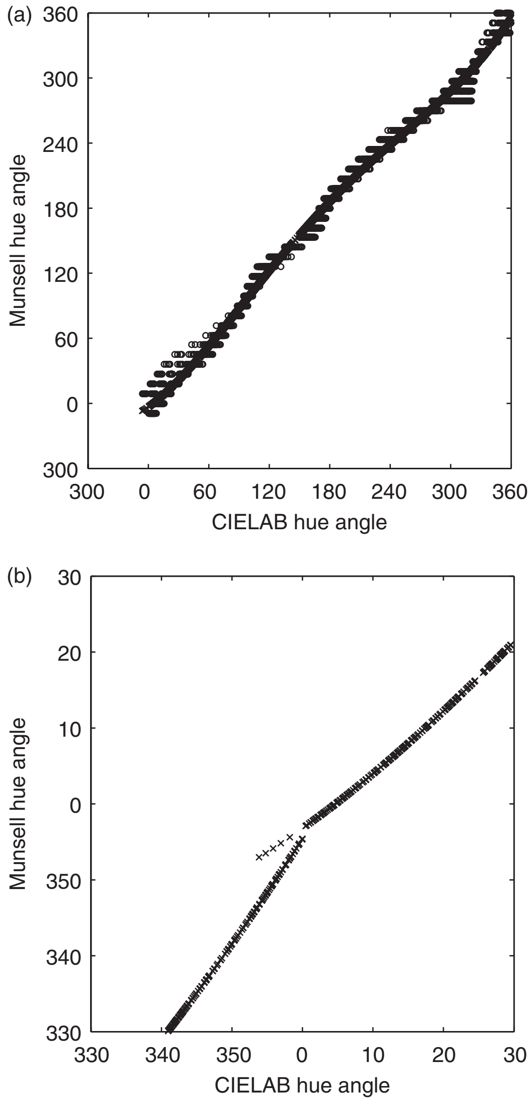

Figure 5 (a) Munsell hue angles against CIELAB hue angles with fitting a fourth-order polynomial (Eqn 4) and (b) magnified image

and the other 2728 samples were selected as the domain from which the LUT or polynomial was constructed. The procedure was repeated 2729 times, leaving a different sample out in each case. To quantify performance, the absolute difference between the identified Munsell hue of the test colour and the predicted Munsell hue was

Table 2 Values of the coefficients in the Eqns 1–7

	Eqn 1	Eqn 2	Eqn 3	Eqn 4	Eqn 5	Eqn 6	Eqn 7
a	0.9754	−0.0005	0.0000008	0.00000004	0.0841	−0.2840	0.7208
b	0.9473	1.1724	−0.00096	−0.00003	−0.0569	−0.0781	−0.0786
c		−11.3626	1.2327	0.0062	0.9815	1.1177	1.1141
d			−13.0634	0.6596	−1.4905	0.0002	−0.0174
e				−3.2203		−0.0008	−0.0007
f						−0.0006	−0.0003
g						0.0020	0.00009
j						0.0014	−0.0781
k						0.0002	−0.0000008
m						2.0970	0.00001
n							0.00001
p							−0.000004
r							0.00002
s							0.00000007
t							0.000003
u							−0.000004
w							12.0184

measured and denoted as ΔH. In each transformation fitting method, the RMS error has been calculated as:

$$\text{RMS error} = \left(\sum(\text{Munsell H} - \text{predicted Munsell H})^2/2729\right)^{1/2} \tag{11}$$

Tables 3 and 4 show the quantitative results for Approach 1 and Approach 2, respectively. The values of maximum, median, standard deviation (SD) of ΔH values and RMS error have been calculated in each transformation method. As shown in Table 3, Eqn 4 gives the best results in Approach 1. However, even Eqn 4 cannot accurately predict Munsell hue in some cases, as evidenced by the high value of the maximum error. Of course, a further reason for rejecting all the methods in Approach 1 is the problem of discontinuity which is illustrated in Figures 2–5.

Table 4 compares all the fitting methods in Approach 2. Although the maximum ΔH in Eqn 5 is less than for the other methods, Eqns 6 and 7 give a lower median value for ΔH and smaller RMS error in comparison with the other methods in Approach 2. It is notable that the results having been taken by Eqn 4 are still the best among all transformation methods. Although at first glance it may appear that Eqn 5 must fit the data better than Eqn 1, for example, as Eqn 1 is a subset of Eqn 5, this would only be true if we were not employing a test set of data. For any given set of data, it is true that the RMS error for Eqn 5 must be equal or lower than that for Eqn 1. However, the use of the leave-one-out error method constitutes the use of training and test data and it is the performance on the test data that is reported in Tables 3, 4 and 5. For example, Eqns 5, 6 and 7 could be over-fitting the training data.

Table 5 demonstrates the performance of the LUT approach (Approach 3) with different criteria (M-1 to M-3) in the calculation of the distance between the target and each of the 2729 Munsell renotation data. As shown in Table 5, in terms of either RMS error or median error, the LUT methods perform better than the best-performing polynomial methods especially, when the distance between the target and Munsell renotation data are calculated using the CIEDE2000 equation. This is consistent with what is known about the abilities of the various equations used in M-1, M-2 and M-3 to accurately predict colour differences.

Table 3 Comparison of different fitting equations in Approach 1

	Eqn 1	Eqn 2	Eqn 3	Eqn 4
Maximum	34.74	31.40	31.28	28.53
Median	6.89	4.55	4.46	4.01
SD	5.47	5.16	5.18	4.53
RMS	9.43	7.79	7.76	6.92

Table 4 Comparison of different fitting equations in Approach 2

	Eqn 5	Eqn 6	Eqn 7
Maximum	24.88	43.03	37.82
Median	6.89	4.13	4.35
SD	4.99	5.10	5.23
RMS	9.05	7.32	7.67

Table 5 Comparison of different methods in LUT model between $L^*C^*_{ab}h_{ab}$ and Munsell H

	M-1 (ΔE^*_{ab})	M-2 (ΔE_{xyz})	M-3 (ΔE_{00})
Maximum	12.37	25.27	10.40
Median	1.62	2.21	1.00
SD	1.84	3.03	1.70
RMS	2.79	4.32	2.37

Application of LUT on the basis of the M-3 method, in which the distance between the target and Munsell renotation data are calculated in accordance to the CIEDE2000 colour-difference equation, was found to be the best method to predict Munsell hue.

Conclusion

Examination of several approaches of transformation of CIELAB coordinates to Munsell hue shows that the construction of a distance-weighted LUT model between 2729 Munsell renotation colour samples is effective and produces the best performance. Various distance-metrics were evaluated for the LUT model and the best performance was given using the CIEDE2000 colour-difference equation. This work has focused on the conversion of CIELAB values to Munsell hue. Existing methods are available to convert CIE values to Munsell value and *vice versa* [3,4,22]. However, work is still required to be able to convert CIE values into Munsell chroma and this should be the topic of further research. In this work, we have shown that LUTs perform better than polynomial transforms; however, just as important was the relative performance of the LUTs using Euclidean distance in XYZ space, CIELAB colour difference and CIEDE2000 colour difference with the latter giving the best performance. This is not entirely surprising given the relative merits of these spaces and equations to predict colour difference. However, it does suggest that further work could be instigated using colour-appearance models such as CIECAM02 [25].

One issue that we have not explored is possible inversion of the model. Very few – if any – of the methods that we have employed would easily lend themselves to inversion. However, we see no reason why the use of LUTs could not be constructed to predict CIELAB h_{ab} from Munsell hue. However, we accept that the use of two LUTs in this way would not be truly invertible in a mathematical sense.

This work was motivated by a need to be able to predict Munsell hue from CIELAB h_{ab} in order that some psychophysical experiments concerned with colour harmony could be correctly and extensively analysed [17]. Without this study, the colour harmony work that we have been working towards would not have been possible and we hope that the publication of our methods in this paper will similarly assist other researchers.

References

1. S M Newhall, *J. Opt. Soc. Am.*, **33** (1943) 385.
2. W C Rheinboldt and J P Menard, *J. Opt. Soc. Am.*, **50** (8) (1960) 802.
3. C S McCamy, *Col. Res. Appl.*, **17** (3) (1992) 205.
4. F T Simon and J A Frost, *Col. Res. Appl.*, **12** (5) (1987) 256.
5. M Miyahara and Y Yoshida, *Vis. Commun. Image Process.*, **1001** (1988) 650.
6. H Laamanen, T Jaaskelainen and J Parkkinen, *Col. Res. Appl.*, **31** (1) (2006) 57.
7. A K Romney and J T Fulton, *Proc. Natl Acad. Sci. USA*, **103** (42) (2006) 15698 (available at: http://www.pnas.org/content/103/42/15698.full) (accessed on 6 December 2009).
8. Y Nayatani, *Col. Res. Appl.*, **29** (2) (2004) 151.
9. N S Smith and J W Billmeyer, Jr., *Col. Res. Appl.*, **22** (2) (1997) 111.
10. A K Romney and T Indow, *Col. Res. Appl.*, **28** (3) (2003) 182.
11. R G Kuehni, *Col. Res. Appl.*, **27** (1) (2007) 20.
12. T Indow, *Col. Res. Appl.*, **24** (1) (1999) 10.
13. T Indow, *Col. Res. Appl.*, **24** (1) (1999) 19.
14. G Marcu, *Proc. IS&T/SID 6th Col. Imaging Conf.*, Scottsdale, USA (1998) 159.
15. R G Kuehni, *Col. Res. Appl.*, **24** (1) (1999) 33.
16. F T Simon, in *Color Measurement*, *Optical Radiation Measurement*, Vol. 2, Eds F Grun and C J Bartleson (New York: Academic Press, 1980).
17. F Mahyar, V Cheung, S Westland and P M Henry, *Proc. AIC Midterm Meeting*, Hangzhou, China (2007) 82.
18. F Mahyar, S Westland and V Cheung, *Proc. AIC Interim Meeting*, Stockholm, Sweden (2008).
19. A K R Choudhury, *Modern Concepts of Color and Appearance* (Enfield: Science Publisher Inc., 2000).
20. Munsell Color Science Laboratory, *Colour Book* (available at: http://www.cis.rit.edu/mcsl/online/munsell.php) (accessed on 6 December 2009).
21. H R Kang, *Color Technology for Electronic Imaging Devices* (Bellingham: SPIE, 1997).
22. R G Kuehni, *Color Space and its Divisions* (Hoboken: John Wiley & Sons Inc., 2003).
23. R Balasubramanian and M S Maltz, *Proc. SPIE*, **2658** (1996) 334.
24. J Morovic and M R Luo, *Proc. IS&T/SID 4th Col. Imaging Conf.*, Scottsdale, USA (1996) 70.
25. N Moroney, M D Fairchild, R W G Hunt, C Li, M R Luo and T Newman, *Proc. IS&T/SID 10th Col. Imaging Conf.*, Scottsdale, USA (2002) 23.

